Retention of Co(II), Ni(II), and Cu(II) on a Purified Brown Humic Acid. Modeling and Characterization of the Sorption Process

Ramón A. Alvarez-Puebla,† Cristóbal Valenzuela-Calahorro,‡ and Julián J. Garrido*,†

Department of Applied Chemistry, Public University of Navarra, Campus Arrosadía, E-31006 Pamplona, Spain, and Department of Inorganic Chemistry, Faculty of Pharmacy, University of Granada, E-18071 Granada, Spain

Received December 9, 2003. In Final Form: January 30, 2004

Brown humic acids (BHAs) constitute the most polar and soluble fraction of humic acids. Their colloidal character and their high number of functional surface groups justify their higher reactivity as against metallic cations with respect to other humic fractions (i.e., gray humic acids and humins). The aim of this work is to study the retention mechanisms of Cu(II), Ni(II), and Co(II) on a BHA by means of a proper combination of physical and chemical techniques: sorption isotherms, mathematical modeling of these isotherms, molecular modeling, FTIR, and N_2 (77 K) and CO_2 (273 K) adsorption. Electrostatic retention for the three cations is an important mechanism at very low concentrations. Its magnitude is higher than that of the specific retention in the initial stages of the retention but it decreases progressively with respect to the former as the initial metal concentration increases. The BHA surface area varies with the amount of retained metal. When the initial amount of added metal is low (n_0 < 80 mmol kg^{-1}), the cations form 2:1 complexes, which are energetically favored due to the chelate effect. To obtain this coordination, the BHA slightly modifies its conformation by decreasing its area. When the initial amount of added metal is sufficiently high to occupy most of the surface functional groups (n_0 > 1280 mmol kg^{-1}), the cations are heterogeneously retained over the whole surface, thus preventing the available groups at low n_0 from giving place to the 2:1 complexes due to the fact that they are already occupied.

Introduction

Humic substances (HSs) are not estequiometric chemical species but macromolecular colloidal phases composed of fulvic, humic, and humin fractions.[1] Their composition is variable and differs sensibly from one sample to another.[2] Brown humic acids (BHAs) constitute the most polar and soluble fraction of humic acids due to their high content in carboxylic and phenolic acidic groups. The presence of these functional groups justifies both the increase in their solubility with pH[3] (they are practically insoluble at pH ≤ 2 and completely soluble at pH ≥ 7) and the higher reactivity versus metallic cations with respect to other humic fractions (i.e., gray humic acids and humins).[4]

Due to their colloidal character, the HS are good adsorbents for a great number of molecular and ionic substances. This gives these substances a key role in the retention and mobilization of nutrients and pollutants in the environment. The interactions between the different metallic species and a solid adsorbent can be deduced from the systematical and coordinated study of the behavior of the metal ions in solution (speciation diagrams versus pH) and of the adsorption and precipitation processes of the metal ion with the reactive functional groups of the solid (sorption isotherms). The sorption isotherm analysis needs to fit the experimental information to a mathematical model. In the bibliography, there are equations of a diverse nature that have been used to fit the sorption isotherms.[5,6] In a previous paper,[7] it has been shown that it is possible to fit the sorption information to a model that postulates the existence of a certain global process with physical chemistry justification, constituted by one or more single adsorption processes.

The sorption isotherm analysis allows the obtainment of macroscopic information of the process.[8,9] Nevertheless, the experimental verification of the hypotheses established in the interpretation of the isotherms needs additional spectroscopic information.[8] For that reason FTIR was used in order to determine the specific interactions of the Cu(II) species with surface functional groups of BHA.[7,10,11] This technique provides information about the changes in the surface functional groups of the BHA. On the other hand, the effect of the metal uptake on the surface texture has been studied by means of N_2 (77 K) and CO_2 (273 K) adsorption isotherms and the electrostatic retention and the conformational changes associated have been explored by using computational techniques.

The aim of this paper is to model isotherms and combine adsorption data with FTIR, N_2 (77 K) and CO_2 (273 K) adsorption, and molecular modeling techniques in order

* To whom correspondence should be addressed. E-mail: j.garrido@unavarra.es. Telephone: 34-948-169601. Fax: 34-948-169606.

† Public University of Navarra.

‡ University of Granada.

(1) Swift, R. S. *Soil Sci.* **1999**, *164*, 790−802.

(2) Stevenson, F. J. *Humus chemistry*: *Genesis, composition and reactions*; John Wiley & Sons: New York, 1994.

(3) De Wit, H. A.; Kotowski, M.; Mulder, J. *Soil Sci. Soc. Am. J.* **1999**, *63*, 1141−1148.

(4) Ghosh, R.; Banerjee, D. K. *Chem. Speciation Bioavailability* **1997**, *9*, 15−19.

(5) Hinz, C. *Geoderma* **2001**, *99*, 225−243.

(6) Tipping, E. *Cation binding by humic substances*; Cambridge University Press: Cambridge, 2002.

(7) Alvarez-Puebla, R. A.; Valenzuela-Calahorro, C.; Garrido, J. J. *J. Colloids Interface Sci.* **2004**, *270*, 47−55.

(8) Sposito, G. *The surface chemistry of soils*; Oxford University Press: New York, 1984.

(9) Sparks, D. L. *Environmental soil chemistry*; Academic Press: San Diego, CA, 1995.

(10) Lu, X. Q.; Vassallo, A. M.; Johnson, W. D. *J. Anal. Appl. Pyrolysis* **1997**, *43*, 103−114.

(11) Piccolo, A.; Stevenson, F. J. *Geoderma* **1982**, *27*, 195−208.

10.1021/la0363231 CCC: $27.50
Published on Web 03/24/2004

to study the Co(II), Ni(II), and Cu(II) retention on a purified BHA. This global aim may be outlined as follows: (a) measurement of M(II) adsorption isotherms on BHA at pH 2; (b) fitting the experimental data to a model that assesses the chemistry of metal ions in aqueous solution and the global adsorption as the sum of several single processes; and (c) characterization of the surface-retained species by using FTIR, N_2 (77 K) and CO_2 (273 K) adsorption, and molecular modeling techniques.

Theoretical Basis

The sorption isotherms of transition metals on HS do not adequately fit the Langmuir equation.[7,12,13] This probably means that several single processes may compose the global retention process. This would seem to be logical considering the different species that can form the metallic cations in solution as a function of pH and metal concentration.[14] The following equations for a divalent transition metal ion as a function of pH have been assumed[15] (in all the cases it has been assumed that M(II) has a coordination number of 6,[16] and we have not considered the oligomeric species)

$$[M(H_2O)_6]^{2+} + OH^- \leftrightarrows [M(OH)(H_2O)_5]^+ + H_2O \quad (1)$$

$$[M(OH)(H_2O)_5]^+ + OH^- \leftrightarrows [M(OH)_2(H_2O)_4] + H_2O \quad (2)$$

$$[M(OH)_2(H_2O)_4] \leftrightarrows M(OH)_2\downarrow + 4H_2O \quad (3)$$

Bearing in mind that most of the cation exchangers have selective behavior as a function of the pH and concentration of the different species, the retention of a metal ion on a BHA could be described by a model that assumes different binding mechanisms.[7] In the experimental conditions described above, four different simple retention processes can take place:

Process 1.

Electrostatic retention of the cation $[M(H_2O)_6]^{2+}$

$$S{-}H + [M(H_2O)_6]^{2+} \leftrightarrows SH{-}[M(H_2O)_6]^{2+} \quad (4)$$

Process 2.

Surface complexation of the cation $[M(H_2O)_6]^{2+}$

$$2S{-}H + [M(H_2O)_6]^{2+} \leftrightarrows [MS_2(H_2O)_4] + 2H_3O^+ \quad (5)$$

Process 3.

Surface complexation of the cation $[M(OH)(H_2O)_5]^+$

$$S{-}H + [M(OH)(H_2O)_5]^+ \leftrightarrows [MS(OH)(H_2O)_4] + H_3O^+ \quad (6)$$

Process 4.

Precipitation of $M(OH)_2$ on the solid surface

$$[M(H_2O)_6]^{2+} + 2OH^- \leftrightarrows M(OH)_2\downarrow + 6H_2O \quad (7)$$

The adsorption processes usually fit to kinetic laws like

$$-\frac{dC}{dt} = k_a C^n(1-\theta) - k_d\theta \quad (8)$$

where k_a and k_d are the adsorption and desorption rate coefficients, respectively, θ is the coverage surface fraction, and n is the partial order of the process.[17,18]

In the equilibrium, eq 8 easily leads to

$$\frac{n^s}{n_m{}^s} = \theta = \frac{KC^n}{1+KC^n} \quad (9)$$

When $n = 1$ (Langmuir equation conditions)

$$n^s = \frac{Kn_m{}^sC}{1+KC} \quad (10)$$

where n^s is the moles of M(II) adsorbed per mass unit of BHA, $n_m{}^s$ is the retention capacity of HS for M^{2+}, and K is the kinetic equilibrium constant.

When the single experimental adsorption isotherms have a high slope end segment, it could be attributed to a simple multilayer process or, as in this case, to precipitation on the surface of low solubility species. The kinetic law can be expressed using the equation

$$-\frac{dC}{dt} = k_1C^m - k_2n^s \quad (11)$$

which in the equilibrium leads to

$$n^s = (k_1/k_2)C^b = AC^b \quad (12)$$

In the most general case, the adsorption global process consists of the four single processes indicated by eqs 4−7. The experimental isotherms will fit to the next general equilibrium equation

$$n^s = n_1{}^s + n_2{}^s + n_3{}^s + n_4{}^s = \frac{K_1n_{m(1)}{}^sC}{1+K_1C} + \frac{K_2n_{m(2)}{}^sC}{1+K_2C} + \frac{K_3n_{m(3)}{}^sC}{1+K_3C} + AC^b \quad (13)$$

where $n_1{}^s$ and $n_2{}^s$ are the millimoles of M^{2+} adsorbed electrostatically and specifically per kilogram of BHA as $[M(H_2O)_6]^{2+}$, $n^s{}_3$ is the millimoles of M^{2+} adsorbed specifically as $[M(OH)(H_2O)_5]^+$, and $n_4{}^s$ is the millimoles of M^{2+} precipitated as $M(OH)_2$ on the BHA surface.

Experimental Section

Humic Samples. The adsorbent used in this study was purified brown humic acid obtained and purified from a commercial HS (Acros Organics) by using the method proposed by the International Humic Substances Society.[19] BHA characterization included chemical composition by using a Carlo Erba EA

(12) Liu, A.; Gonzalez, R. D. *Langmuir* **2000**, *16*, 3902−3909.
(13) Davies, G.; Fataftah, A.; Cherkasskiy, A.; Ghabbour, E. A.; Radwan, A.; Jansen, S. A.; Kolla, S.; Paciolla, M. D.; Sein, J. L. T.; Buermann, W.; Balasubramanian, M.; Budnick, J.; Xing, B. *J. Chem. Soc., Dalton Trans.* **1997**, *21*, 4047−4060.
(14) Burriel, F.; Lucena, F.; Arribas, S.; Hernandez, J. *Química analítica cualitativa*, 16th ed.; Paraninfo: Madrid, 1998.
(15) Huheey, J. E.; Keiter, E. A.; Keiter, R. L. *Inorganic chemistry. Principles of structure and reactivity*; Harper Collins: New York, 1993.
(16) Xia, K.; Bleam, W.; Helmke, P. A. *Geochim. Cosmochim. Acta* **1997**, *61*, 2223−2235.
(17) Valenzuela-Calahorro, C.; Cuerda-Correa, E.; Navarrete-Guijosa, A.; Gonzalez-Pradas, E. *J. Colloid Interface Sci.* **2002**, *250*, 67−73.
(18) Valenzuela-Calahorro, C.; Cuerda-Correa, E.; Navarrete-Guijosa, A.; Gonzalez-Pradas, E. *J. Colloid Interface Sci.* **2002**, *248*, 33−40.
(19) Swift, R. S. In *Method of soil science analysis*: *Chemical methods*. Part 3; Sparks, D. L., Ed.; Soil Science Society of America: Madison, WI, 1996; pp 1011−1069.

Table 1. Selected Physical and Chemical Properties of the BHA

C (%)	52.3	E_4/E_6	3.49
H (%)	3.95	$\langle M_w \rangle$ (g mol^{-1})[a]	1.14×10^4
N (%)	0.73	$C_{\text{strong acidic groups}}$ (mol kg^{-1})	4.32
S (%)	2.01	$C_{\text{weak acidic groups}}$ (mol kg^{-1})	2.86
ash	*b*	pK_A	3.74
O (%)	41.0	pK_B	7.98

[a] Average molecular weight estimated from $M_w = 3.99\epsilon_{280} + 490$ according to Chin et al.[21] [b] Not detected.

1108 elemental analyzer and UV−vis spectroscopy (Lambda 3B, Perkin-Elmer)[20,21] and acid−base properties. The strong acidic groups and the total acidity of BHA were determined by calcium acetate and barium hydroxide methods,[2] respectively. The weak acidic groups were calculated as the difference between the total acidity and that of the strong acidic groups. The acid−base constants were estimated from the end points obtained from a potentiometric acid−base titration in a Metrohm Titrino 702SM autoburet according to Santos et al.[22] The results of the characterization of the BHA are listed in Table 1.

Adsorption Isotherms. Batch adsorption was carried out using 50 mL scaled centrifuge tubes made out of low-density polyethylene. Samples of BHA 0.2500 ± 0.0005 g were suspended in 20 mL of MilliQ distilled water. The pH was adjusted with the addition of diluted HCl. Suspensions were then placed in a thermostated water bath, Grant OPLS 200, at 298.0 ± 0.2 K during 24 h. The required amount of metal (0, 10, 20, 40, 80, 120, 160, 320, 640, and 1280 mmol kg^{-1}) was added to each sample from a 10 000 ppm solution of $MCl_2 \cdot 6H_2O$ (Merck, analytical grade), and the ionic strength was adjusted to 0.05 M with NaCl 0.25 M solution. The volume was set to 25 mL, and the pH was readjusted. Samples were then placed in the thermostated water bath for 24 h, sufficient time to reach thermodynamic equilibrium, centrifuged for 30 min at 14000*g* (Sigma, model 2-16), and filtered (Millipore, 0.45 μm). The M(II) concentration in filtrates was determined by atomic absorption spectrophotometry (Perkin-Elmer, model 2100), and the amount of metal retained was calculated from the difference between the initial amount and the equilibrium concentration. The residue was vacuum-dried at 338 K. The isotherms at pH 2 were replicated two times, to test the reproducibility of adsorption data.

FTIR Spectroscopy and Gas Adsorption Measurements. Selected samples of the isotherms (doped with 0, 80, and 1280 mmol of M(II) per kg of HS) were studied by FTIR and gas adsorption, with N_2 (77 K) and CO_2 (273 K). For FTIR spectroscopy, the samples were washed three times with ethanol during 5 min, vacuum filtered, vacuum-dried at 333 K for 24 h, and characterized with transmission FTIR (Nicolet, Avatar 360) on KBr pressed pellets (150 mg of KBr and 1 mg of sample). The transmission FTIR cell was flushed with N_2 gas for 10 min before scanning to remove atmospheric water vapor and CO_2 from the spectrophotometer. The spectral resolution was set to 1 cm^{-1}, and 150 scans were collected in each spectrum.

The gas adsorption isotherms were measured with a Micromeritics 2010 by the static volumetric method,[23] the surface area was evaluated by using the Dubinin−Radushkevich (DR) method[24] and the microporous distribution was determined by using the Hovarth−Kawazoe (HK) method[25] on the CO_2 isotherms. For the application of the HK method to HS, the parameters deduced for an active carbon were used as this material is of a similar chemical nature to those kinds of substances.[26]

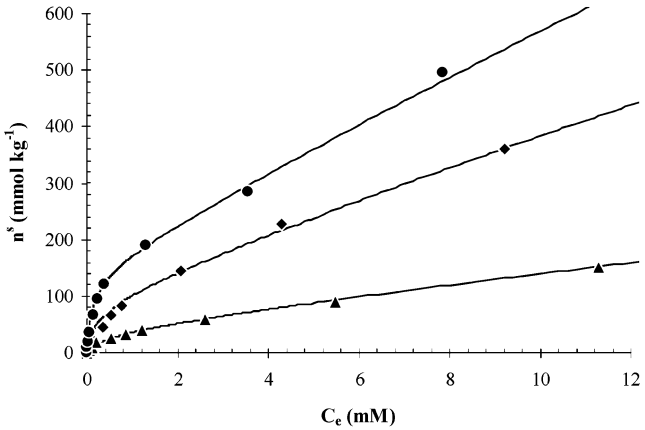

Figure 1. Sorption isotherms at 298 K and pH 2 of Cu(II), Ni(II), and Co(II) on BHA (I = 0.05 M NaCl): (●) Cu(II); (▲) Ni(II); (◆) Co(II); (—) model.

Molecular Modeling. The computational calculations were carried out with HyperChem 7 molecular modeling suite. For the simulation of the electrostatic retention, a polymeric BHA was modeled in accordance with the elemental composition, number of acidic groups, and $\langle M_w \rangle$ (Table 1). The model design was based upon the TNB building block widely used in the bibliography.[13,27−29] The BHA model was obtained by polymerization of 13 modified TNB subunits (previously optimized with molecular mechanics, MM+, and the semiempirical method PM3) with a peptidic bond between NH_2 and COOH groups. The polymeric structure was optimized by using the MM+ force field with the Polak−Ribiere algorithm. In this present study, the convergence limit was set by a maximum acceptable gradient of 0.0418 kJ mol^{-1} nm^{-1}. Quenched dynamic (QD) cycles at 700 K with a step size of 1 fs were performed on the optimized structure in order to explore the conformational space. The most stable local minimum was reoptimized under the same conditions.[30,31] For the docking between BHA and the hexaaquo complex, the system composed of one BHA molecule and one hexaaquo complex was subjected to cycles of molecular dynamics (MD) in the following conditions: 2 ps of warming up to 298 K, 3 ps of stabilization, and 10 ps of simulation, with a time step of 1 fs. Due to the fact that the system is too large to establish periodic boundary conditions, the effect of the dissolvent was considered by applying the Langevin equation for movement[32]

$$m\frac{\mathbf{d}^2}{\mathbf{d}t^2} = -\zeta\frac{\mathbf{d}r}{\mathbf{d}t} + \mathbf{F}_{\text{intramolecular}} + \mathbf{F}_{\text{random}} \qquad (14)$$

where ζ is the friction coefficient, characteristic of each fluid and proportional to the Brownian movement due to the temperature ($\mathbf{F}_{\text{random}}$). $\mathbf{F}_{\text{intramolecular}}$ represents the movement from the intramolecular forces and is, for this reason, characteristic of the system. After every MD cycle, a geometric optimization was carried out on the system by using the Polak−Ribiere algorithm down to a gradient of 0.0418 kJ mol^{-1} nm^{-1}.

Results and Discussion

Sorption Isotherms at pH 2. Figure 1 shows the sorption isotherms for Cu(II), Ni(II), and Co(II) on BHA at pH 2, 298 K, and ionic strength 0.05 M in NaCl. The

(20) Chen, Y.; Senesi, N.; Schnitzer, M. *Soil Sci. Soc. Am. J.* **1977**, *41*, 352−258.
(21) Chin, Y.-P.; Aiken, G.; O'Loughlin, E. *Environ. Sci. Technol.* **1994**, *28*, 1853−1858.
(22) Santos, E. B. H.; Esteves, V. I.; Rodrigues, J. P. C.; Duarte, A. C. *Anal. Chim. Acta* **1999**, *392*, 333−341.
(23) Rodriguez-Reinoso, F.; Garrido, J.; Martin-Martinez, J. M.; Molina-Sabio, M.; Torregrosa, R.*Carbon* **1989**, *27*, 23−32.
(24) Dubinin, M. M.; Radushkevich, L. V. *Zh. Fiz. Khim.* **1949**, *23*, 469.
(25) Hovarth, G.; Kawazoe, K. J. *Chem. Eng. Jpn.* **1983**, *16*, 470.
(26) Webb, P. A.; Orr, C. *Analytical methods in fine particle technology*; Micromeritics Instrument Corporation: Norcross, MA, 1997.
(27) Sein, L. N.; Varnum, J. M.; Jansen, S. A. *Environ. Sci. Technol.* **1999**, *33*, 546−552.
(28) Kubicki, J. D.; Apitz, S. E. *Org. Geochem.* **1999**, *30*, 911−927.
(29) Bruccoleri, A. G.; Sorenson, B. T.; Langford, C. H. In *Humic substances*: *Structures, models and functions*; Gabbour, E. A., Davies, G., Eds.; The Royal Society of Chemistry: Cambridge, 2001; pp 193−208.
(30) Shevchenko, S. M.; Bailey, G. W.; Akim, L. G. *J. Mol. Struct. (THEOCHEM)* **1998**, *460*, 179−190.
(31) Schulten, H. R. *J. Anal. Appl. Pyrolysis* **1999**, *49*, 385−415.
(32) Jensen, F. *Introduction to Computational Chemistry*; Wiley: New York, 1999.

Table 2. Fitted Parameters for Equation 15

	Cu(II)	Ni(II)	Co(II)
$n_{m(1)}{}^s$ (mmol kg^{-1})	9.34	1.90	8.83
K_1	9.00×10^4	9.87×10^4	5.25×10^4
$n_{m(2)}{}^s$ (mmol kg^{-1})	133	32.6	77.3
K_2	6.46	2.10	3.41
$n_{m(3)}{}^s$ (mmol kg^{-1})	4.40×10^3	1.47×10^3	3.59×10^3
K_3	1.06×10^{-2}	7.20×10^{-3}	9.10×10^{-3}
R^2	0.9976	0.9992	0.9979

three isotherms can be included in the L-type according to Giles.[33] All of them show a marked initial slope that decreases as the metal equilibrium concentration increases. These isotherms are the result of a high affinity of BHA for the adsorbates at low metal concentrations, together with a decrease of the available surface functional groups as the solute equilibrium concentrations increases.

According to the speciation diagrams for Cu(II), Ni(II), and Co(II),[14] at pH 2 the principal species present in solution are $[M(H_2O)_6]^{2+}$ and $[M(OH)(H_2O)_5]^{+}$. Therefore, the global sorption process can be treated as the sum of three single processes: (i) electrostatic retention of $[M(H_2O)_6]^{2+}$, according to eq 4; (ii) surface complexation of $[M(H_2O)_6]^{2+}$, according to eq 5; and (iii) surface complexation of $[M(OH)(H_2O)_5]^{+}$, according to eq 6. So, eq 13 reduces to

$$n^s = n_1{}^s + n_2{}^s + n_3{}^s + = \frac{K_1 n_{m(1)}{}^s C}{1 + K_1 C} + \frac{K_2 n_{m(2)}{}^s C}{1 + K_2 C} + \frac{K_3 n_{m(3)}{}^s C}{1 + K_3 C} \quad (15)$$

The experimental data (n^s vs C_e) fit very well to eq 15 to give the results shown in Table 2. The maximum retention capacity ($n_m{}^s = n_{m(1)}{}^s + n_{m(2)}{}^s + n_{m(3)}{}^s$) follows the order: Cu > Co > Ni. Figure 2 shows the speciation diagrams for metal retained on the BHA surface as a function of the initial amount of added metal, deduced from the parameters obtained by applying eq 15 shown in Table 2. The electrostatic retention, just like surface complexation such as hexaaquo complex, provides a curve that begins with a large slope that decreases with the initial amount of added metal as the charge is saturated. In the case of the surface complexation such as $[M(OH)(H_2O)_5]^{+}$ the slope is initially small but increases with n_0. The electrostatic retention is only higher than the surface complexation at very low n_0. The variation of the retention mechanism with n_0 points toward the competition between metallic ions and protons in order to occupy the carboxylic groups.[34,35] This way, as metal is added the ratio M^{2+}/H^{+} increases and consequently the surface complexation increases. Both the electrostatic retention and the surface complexation capacities follow the order Cu > Co > Ni.

Although the kinetic equilibrium constants (Table 2) have no thermodynamic value and cannot be used as a predictive criterion, their values follow the next order $K_1 > K_2 > K_3$. This can be interpreted as a decrease in the speed of adsorption for all three processes. In this way, the electrostatic retention of $[M(H_2O)_6]^{2+}$ is more rapid than the complexation of the same species and this latter is more rapid than the complexation of $[M(OH)(H_2O)_5]^{+}$. This is coherent with the progressive complication in the adsorption process; whereas the electrostatic adsorption only requires the approximation of the adsorbate to the adsorbent, the complexation of the $[M(H_2O)_6]^{2+}$ needs a previous dissociation reaction and a suitable approximation of the metal to its new ligand. In the case of the complexation of $[M(OH)(H_2O)_5]^{+}$, the formation of this species also needs a dissociative substitution reaction.[15]

Comparing the values of the respective equilibrium kinetic constants for the three metals, it can be appreciated that, for the electrostatic retention the order of K_1 is Ni > Cu > Co, whereas for both surface complexation mechanisms (K_2 and K_3) the order is Cu > Co > Ni. Bearing in mind that the electrostatic retention is much lower than surface complexation retention, a higher speed of retention for Cu followed by Co and Ni might be considered. These results are consistent with the bibliography[12,13,36] and the solution chemistry of the three metals. In this way, Cu(II) is the most reactive ion due to the Jahn−Teller effect while Ni(II) is the most inert, due to its high crystal field stabilization energy.[15]

Molecular Modeling of the Electrostatic Retention. Given that the three metals have similar behavior, Figure 3 only shows the results obtained after the simulation of the electrostatic retention of a molecule of $[Co(H_2O)_6]^{2+}$ on BHA. The $[Co(H_2O)_6]^{2+}$ is stabilized by H-bonds with the BHA functional groups of the BHA (carbonyl and hydroxyl groups from −COOH and phenols), generating outer-sphere complexes, as Senesi[37] suggests. The H-bonds not only are limited to a surface group but also bond several groups simultaneously; in fact, the BHA changes its spatial conformation to maximize these interactions with the metal complexes (Figure 3a). It is likely that the electrostatic retention is the previous step for the surface complexation since it increases the effective concentration of metal around the surface functional groups of BHA, which would agree with the information provided by the speciation diagrams (Figure 2).

Figure 3b shows the variation of the potential energy as a function of the distance in the formation of the first H-bond between $[Co(H_2O)_6]^{2+}$ and BHA. The electrostatic retention is a weak exothermic process, as corresponds to the kind of interactions that take place on the system. The equilibrium distance is about ∼0.4 nm; as the aquo complex moves away from this point, the energy increases exponentially when it approaches the BHA, as a consequence of the intermolecular repulsions, and linearly when it moves away from it, as a consequence of the electrostatic attraction.

Cobalt retention also modifies the textural properties of the molecule. The van der Waals area (3620 m^2 g^{-1}), calculated according to Gavezzoti,[38] decreases 4.5% when $[Co(H_2O)_6]^{2+}$ is added as a consequence of the distortion in the conformation that the macromolecule contracts in order to maximize the weak bonding forces with Co complex. This has been already described by some authors,[39,40] who relate it to the aggregation phenomena of HS induced by the high ionic strength.

Effect of the Metal Uptake on the BHA Porosity. The BHA porous texture was explored using adsorption isotherms of N_2 (77 K) and CO_2 (273 K) (Table 3). The molecular size of both adsorbates is similar (0.30 and 0.33 nm, respectively). However, the sample adsorbed CO_2 but

(33) Giles, C. H.; MacEwan, T. H.; Nakhwa, S. N.; Smith, D. *Chem. Soc.* **1960**, 3976−3993.
(34) Breault, R. F.; Colman, J. A.; Aiken, G. R.; McKnight, D. *Environ. Sci. Technol.* **1996**, *30*, 3477−3486.
(35) Choi, I. S.; Okazaki, M.; Yamaguchi, N. U. *Soil Sci. Plant Nutr.* **1999**, *3*, 527−535.
(36) Mandal, R.; L. R. Sekaly, A.; Murimboh, J.; Hassan, N. M.; Chakrabarti, C. L.; Back, M. H.; Gregoire, D. C.; Schroeder, W. H. *Anal. Chim. Acta* **1999**, *395*, 323−334.
(37) Senesi, N. In *Biogeochemistry of trace metals*; Adriano, D. C., Ed.; Lewis: Boca Raton, FL, 1992; pp 429−496.
(38) Gavezzotti, A. *J. Am. Chem. Soc.* **1983**, *105*, 5220−5225.
(39) Senesi, N. *Soil Sci.* **1999**, *164*, 841−856.
(40) Tombacz, E. *Soil Sci.* **1999**, *164*, 814−824.

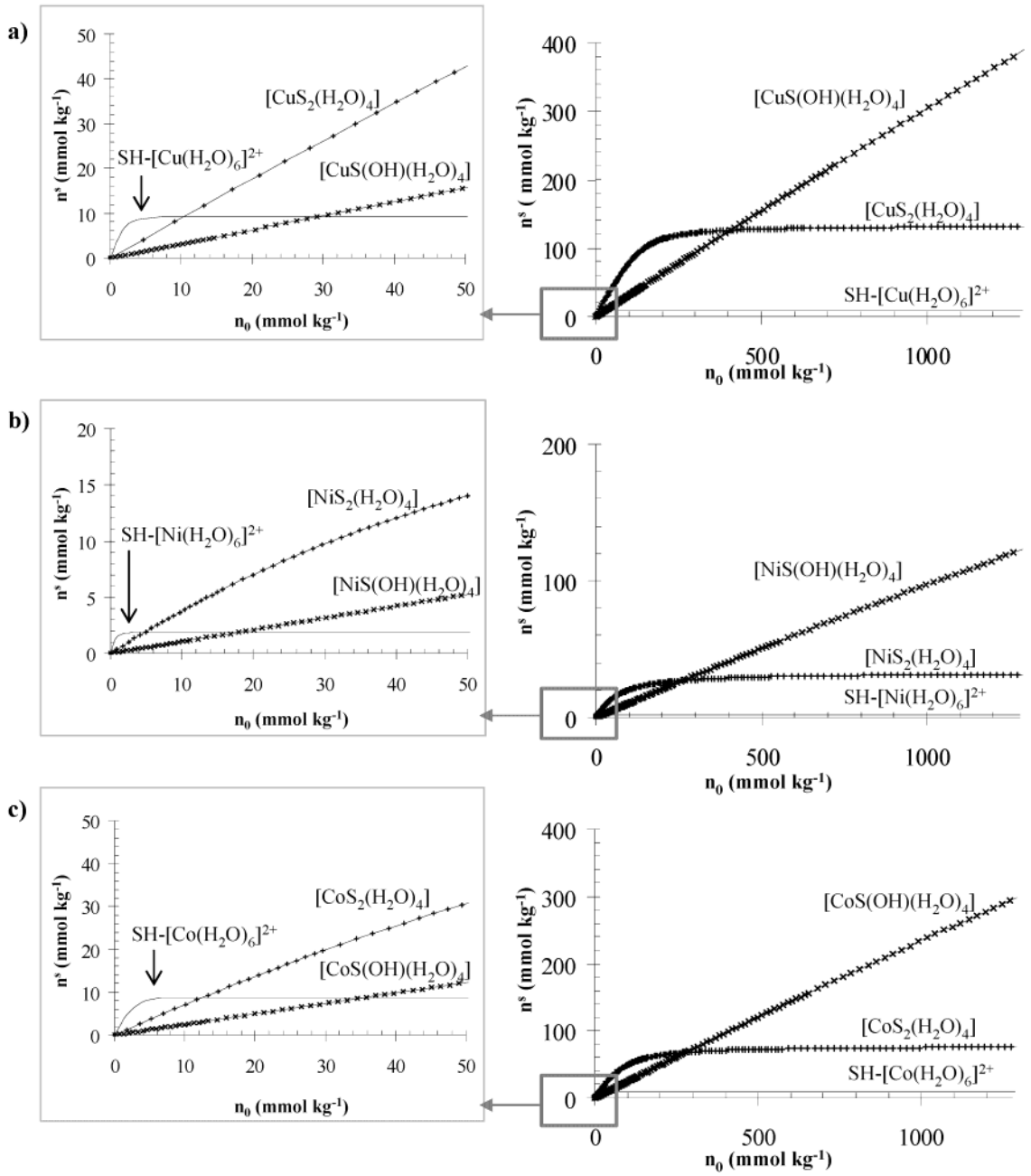

Figure 2. Surface speciation diagrams of metal retained on BHA as a function of initial amount of added metal obtained applying eq 15 for (a) Cu(II), (b) Ni(II), and (c) Co(II) (pH 2, I = 0.05 M NaCl, and 298 K).

no N_2 was retained, which can be explained by the extremely narrow microporosity of this kind of material. Whereas CO_2 can penetrate the micropores, N_2 cannot, due to diffusion restrictions because of its lower kinetic energy at 77 K.[41,42]

Figure 4 shows the CO_2 (273 K) adsorption isotherms for selected points of the Cu, Ni, and Co on BHA isotherms. The quantity of adsorbed CO_2 and so the surface area (Table 3) decreases when a small amount of metal is added but increases when the amount of added metal is large. However, the area is always lower than that of the undoped sample. This fact may be because when the initial amount of added metal is low (80 mmol kg^{-1}), the competition of the BHA surface functional groups to complex metal takes place, fundamentally, to complexes 2:1, in agreement with eq 5. As the amount of added metal increases, the competition decreases, so at sufficiently high concentrations (1280 mmol kg^{-1}) the BHA tends to form 1:1 complexes, in which the positive remaining charge is neutralized by the coordination of an hydroxyl group in agreement with eq 6. To sum up, although the 2:1 complexes are thermodynamically more stable due to the chelate effect,[15,43] their formation is impeded due to a shortage of suitable surface groups, which are already complexed with the metal, giving place to a minor compacting structure and, therefore, a larger surface area than that in the previous case.

The HK micropore distributions (Figure 5) show that when BHA retains the metal ions, the amount of certain

(41) Garrido, J.; Linares-Solano, A.; Martin-Martinez, J. M.; Molina-Sabio, M.; Rodriguez-Reinoso, F.; Torregrosa, R. *Langmuir* **1987**, *3*, 76−81.

(42) Echeverria, J. C.; Morera, M. T.; Mazquiaran, C.; Garrido, J. J. *Eur. J. Soil Sci.* **1999**, *50*, 497−503.

(43) Naidu, R.; Harter, R. D. *Soil Sci.* **1998**, *62*, 644−650.

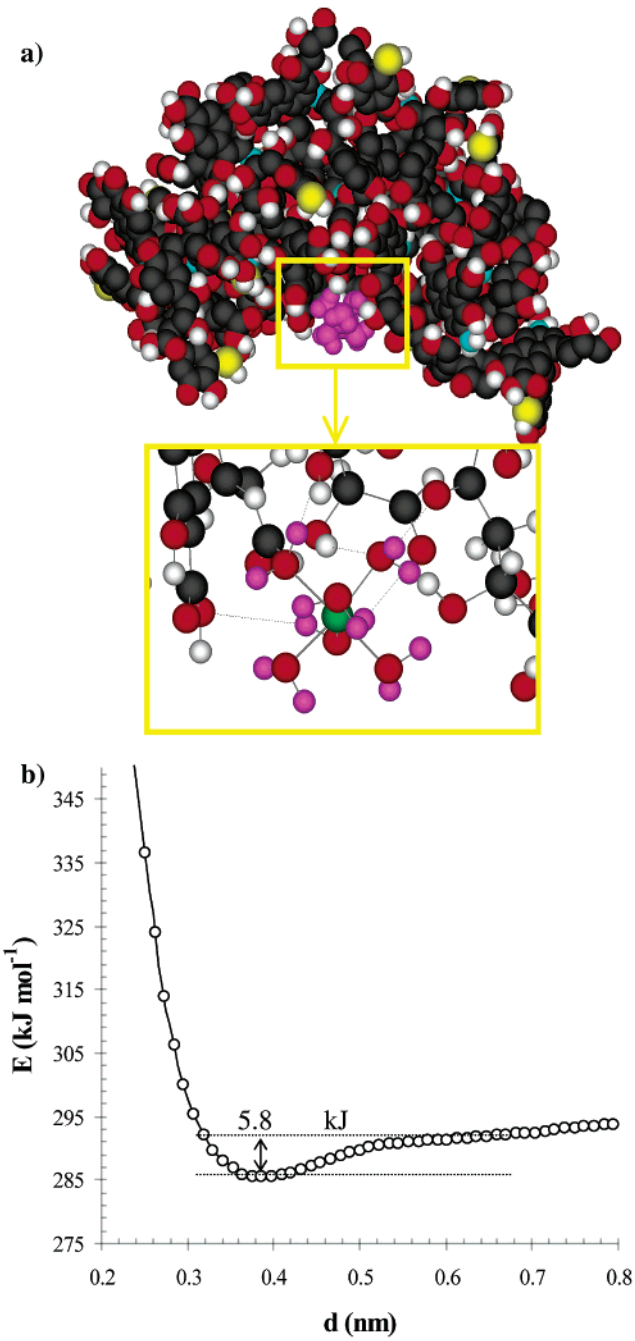

Figure 3. (a) Structure of a BHA−$[Co(H_2O)_6]^{2+}$ complex as inferred from molecular mechanics modeling: O, red; H, white; N, blue; S, yellow; C, black; $[Co(H_2O)_6]^{2+}$, violet (the enlargement shows the H-bonds (dotted lines)); Co^{2+}, green; H_2O, violet. (b) Potential energy variation as a function of the distance during the formation of the first H-bond between $[Co(H_2O)_6]^{2+}$ and BHA.

Table 3. BHA Surface Area Values as a Function of the Initial Amount of Added Metal Obtained by Applying Dubinin−Radushkevish Method to the CO_2 (273 K) Isotherms

	A_s (m^2 g^{-1})		
n_0 (mmol kg^{-1})	Cu(II)	Ni(II)	Co(II)
0	88.0	88.0	88.0
80	46.4	56.1	48.1
1280	65.0	74.7	61.4

porous sizes varies. The undoped BHA shows four maxima at 0.36, 0.38, 0.44, and 0.54 nm. In all the cases, the maximum placed at 0.44 nm is supported; the maximum placed to 0.36 nm is supported in the samples doped with 1280 mmol kg^{-1} but disappears in the samples doped with 80 mmol kg^{-1}, which is in line with the previous hypothesis. The disappearance of a certain type of micropores when the amount of retained metal is low, and the conservation of this porosity when it is high implies that the metals, at low concentrations, influence the three-dimensional conformation of BHA more than at high concentrations. To obtain a 2:1 coordination, the BHA slightly modifies its conformation, eliminating some pores. When n_0 is high enough, the cations occupy most of the surface functional groups and therefore inhibit the formation of 2:1 complexes. In conclusion, high concentrations of metal preserve the three-dimensional structure of BHA. On the other hand, the similarity in the micropore distributions for the three metals suggests that the retention mechanisms in the experimental conditions are similar, which agrees with the information obtained in the speciation.

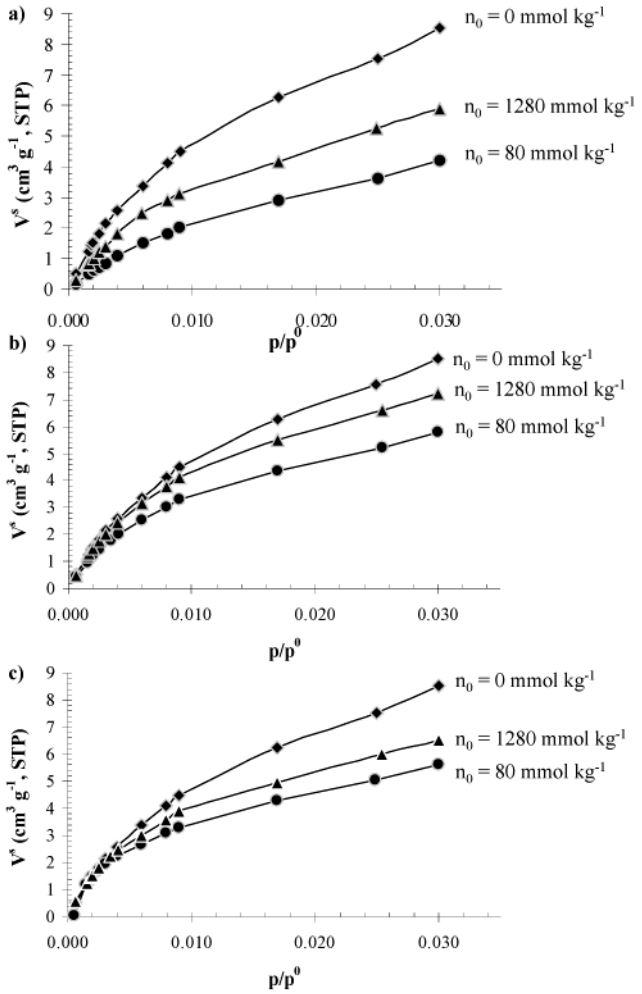

Figure 4. CO_2 (273 K) sorption isotherms for (a) BHA−Cu(II), (b) BHA−Ni(II), and (c) BHA−Co(II) for selected samples from the isotherms (0, 80, and 1280 mmol kg^{-1}).

FTIR Characterization of the Metal Uptake by BHA. Figure 6 shows the FTIR spectra for residues of selected points from the sorption isotherms of Cu, Ni, and Co on BHA. All spectra of the doped samples show characteristic variations in their bands due to the retention of metal ion aquo complexes: (i) increasing the intensity of ν(O−H) band (~3420 cm^{-1}) due to the absorption of the water of the retained aquo complexes;[37] (ii) decreasing in the intensity of ν(C═O) band of −COOH (~1720 cm^{-1}) and ν(C−O) and ρ(O−H) bands (~1240 cm^{-1}); (iii) increasing the bands assigned to the asymmetric and

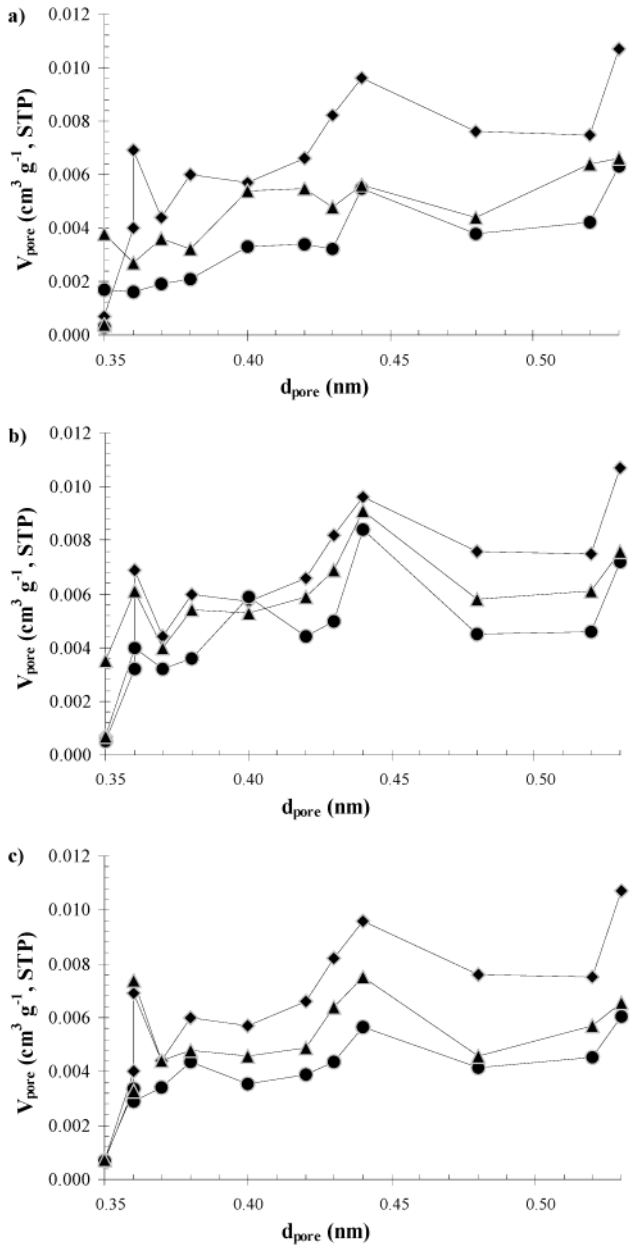

Figure 5. Howarth−Kawazoe micropore distributions for (a) Cu, (b) Ni, and (c) Co, doped with an initial amount of metal of (◆) 0, (●) 80, and (▲) 1280 mmol kg^{-1}.

symmetric −COO$^-$ stretching (∼1600 and ∼1380 cm^{-1});[37] and (iv) decreasing the intensity of the shoulder placed at ∼2600 cm^{-1}, assigned to *ν*(O−H) of H-bonded −COOH.

The higher variations are found in samples doped with a greater amount of metal. In these samples there is an appreciable increase in the bands at ∼3420, ∼1620, and ∼1380 cm^{-1} and a decrease of intensity in those placed at ∼1710 and ∼1240 cm^{-1}, which indicates that the metal is retained by surface complexation according to eqs 5 and 6. The samples doped with 80 mmol kg^{-1} show lower variations. All the samples present an increase of *ν*(O−H), but only the samples doped with Cu(II) and Co(II) show a slight decrease in the intensities of the bands placed at ∼1710 and ∼1240 cm^{-1}, which indicates that at this concentration the electrostatic retention plays a key role in the global retention process.

Taking the three metals into consideration, the samples doped with copper show the most significant variations, followed by Co(II) and Ni(II), in line with the amount of metal retained. The variations in the sample doped with 1280 mmol kg^{-1} of Cu(II) are so great that the spectra show bands that were overlapped in BHA like aromatic C−H stretching (3020 cm^{-1}) or the −C−OH stretching due to aliphatic alcohols and C−O stretching assigned to alcohol and ethers (1100 cm^{-1}). These facts are due to the gradual decrease of the intensities because of the formation of mixed complexes between Cu(II) and COOH groups from the BHA, H_2O, and OH^-.

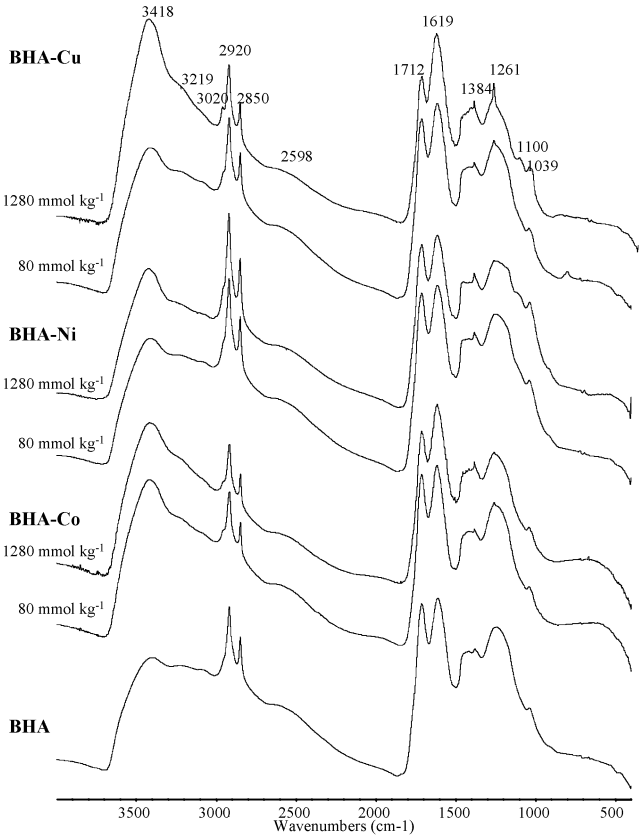

Figure 6. FTIR spectra of BHA and BHA doped with Cu(II), Ni(II), and Co(II) (80 and 1280 mmol kg^{-1}).

All of these variations are consistent with the speciation diagrams (Figure 2) and so they support the hypothesis on which the model described by eq 15 is based.

Conclusions

According to the model used for the isotherm modeling, the electrostatic retention is an important retention mechanism at very low concentrations, where its magnitude is larger than that of the surface complexation in the initial stages of the retention but where it progressively decreases as the initial amount of added metal increases. This hypothesis is supported by FTIR and its likely explanation is that electrostatic retention is the first step of the surface complexation retention since it increases the effective concentration of metal around the surface functional groups of BHA. This hypothesis is also consistent with the molecular modeling simulation of the electrostatic retention.

The retention capacity follows the order Cu > Co > Ni. The BHA shows higher affinity for Cu, followed by Co and Ni. These results are consistent with the bibliography and the solution chemistry of the three metals. Thus, Cu(II) is the most reactive ion due to the Jahn−Teller effect while Ni(II) is the most inert due to its high crystal field stabilization energy.

The BHA surface area varies with the amount of metal retained. This fact may be due to both the higher stability of the 2:1 complexes (due to the chelate effect) and the discontinuous preparation method of isotherms. When the initial concentration of metal is sufficiently high the cations complex most of the BHA functional groups and inhibit the formation of 2:1 complexes.

LA0363231